J Mater Sci: Mater Electron (2017) 28:11415–11419
DOI 10.1007/s10854-017-6936-0

Suppression of the order–disorder transition in Ti-doped YBaCuO compounds

S. V. Savich [1] · A. V. Samoylov[1] · S. N. Kamchatnaya[1] · O. V. Dobrovolskiy[2] · R. V. Vovk[1] · A. L. Solovjov[3,4] · L. V. Omelchenko[3,4]

Received: 16 February 2017 / Accepted: 8 April 2017 / Published online: 19 April 2017

Abstract The influence of titanium impurities on the magnetoresistance of $YBa_2Cu_3O_{7-\delta}$ ceramics near the superconducting transition is investigated in magnetic fields up to 7 T. The mechanisms for low-temperature resistance "tails" (paracoherent transitions) to appear are discussed in the context of different states of vortex matter in the samples. At temperatures above T_c, the temperature dependence of the excess conductivity is satisfactory described within the framework of the Aslamazov–Larkin model for the fluctuation conductivity of layered superconductors.

1 Introduction

The discovery of high-temperature superconductors (HTSCs) in 1986 [1] is known to have triggered a plenty of expectations for their practical use at temperatures above the nitrogen liquefaction temperature, in particular, for high magnetic field applications. However, as it has later on been revealed, a short coherence length [2–4] along with a large penetration depth [5, 6] in conjunction with the presence in the system of pronounced thermal fluctuations lead to that the thermally activated flux creep is observed in HTSCs at temperatures substantially below the critical temperature, $T \ll T_c$ [7, 8]. At the same time, the depinning processes in the vortex subsystem in HTSCs take place much more intensively [5] than in conventional low-temperature superconductors. In consequence of this the latter have been taking the rag off for high-field applications. At the same time, in the last years there have been substantial developments in increasing the critical current density in various HTSC compounds, primarily owing to the optimization of their content and the morphology of the ensemble of defects [5, 9, 10].

In this work, the results of investigations of the influence of Ti on the magnetoresistance of YBaCuO ceramics is presented. The choice of the latter as an object of the study is stipulated by the following reasons. First, at present YBaCuO ceramics are most easy-to-use ones [11, 12] thanks to the relative simplicity of their fabrication and a high transition temperature [13]. Second, this compound is characterized by one of the highest in YBCO compounds critical current densities [5, 9]. Third, the presence of grain boundaries, hindering the diffusion of the labile component, contributes to the stability of the oxygen subsystem in the course of long-term exploitation and aging [12, 14, 15]. Finally, the addition of Ti impurities does not often lead to the replacement of the constituents that is likely to further the formation of additional pinning sites. Due to the small coherence length in the given YBCO compound, the latter can also be very efficient for fine-sized defects such as oxygen vacancies [16, 17] and inclusion impurities [5, 18]. Given the stated above, here we investigate the effect of Ti impurities on the magnetoresistive characteristics of ceramic YBaCuO compounds in the region of the transition to the superconducting state.

✉ O. V. Dobrovolskiy
Dobrovolskiy@Physik.uni-frankfurt.de

[1] V. N. Karazin National University, Kharkiv, Ukraine

[2] Physikalisches Institut Goethe University, Frankfurt am Main, Germany

[3] B. Verkin Institute for Low Temperature Physics and Engineering, Kharkiv, Ukraine

[4] International Lab of High Magnetic Fields and Low Temperatures, Wrocław, Poland

2 Experiment

2.1 Crystal growth

The $YBa_2Cu_3O_{7-\delta}$ samples were synthesized from Y_2O, $BaCO_3$ and CuO, taken in the respective molar relations, in the temperature interval 750 − 900 °C. The obtained powder was crimped at a pressure of ≃4 GPa into Ø20 × 4 mm^2 cylinders and was sintered at a temperature of 950–970 °C for 5 h followed by subsequent cooling to room temperature with intermediate 2–3 h long aging at 890 and 530 °C. The cylinders thus obtained are superconducting ceramics with a rhombic lattice symmetry and $T_c \simeq 90$ K. To obtain samples with titanium impurities, various amounts of weight percent of TiO_2 were added to the initial batch. The fabrication and oxygen saturation procedures were the same as for the impurity-free ceramics.

2.2 Phase composition

The phase composition and the crystal structure of the $YBa_2Cu_3O_{7-\delta}$ ceramics were analyzed by X-ray diffraction with Cu K_α. The data were acquired with an angle resolution of $2\theta = 0.1°$ between peaks and $2\theta = 0.02°$ at the positions peaks. The results of the X-ray diffraction measurements are reported in Fig. 1. An analysis of the diffractograms has revealed that the initial sample has an orthorhombic structure of the perovskite type with the following lattice parameters: $a = 3.8348$ Å, $b = 3.8895$ Å and $c = 11.6790$ Å that is in agreement with literature. With increasing content of the Ti oxide the intensity of the Bragg maxima corresponding to the original structure is reduced, while new maxima associated with the perovskite-type orthorhombic structure, but with $a = 4.2027$ Å, $b = 4.2662$ Å and $c = 12.6415$ Å appear. Maxima corresponding to an yttrium phase were also revealed. With increasing content of TiO_2 the peaks related to the original YBCO phase become less pronounced while those corresponding to the new phase increase. This is accompanied by an increase of the magnitude of the (002) yttrium reflex. For all nominal Ti contents above 37.5% one recognizes a peak corresponding to (111) Cu. Therefore, the X-ray data suggest that with increasing Ti content the composition of the original sample is modified as a new phase with an orthorhombic structure of the perovskite type is formed in conjunction with setting apart Y and Cu into separate phases.

2.3 Resistance measurements

The electrical contacts were arranged in the standard four-probe geometry. They were fromed by applying indium on the sample surface followed by the attachment of silver conductors of 0.05 mm in diameter. This procedure has

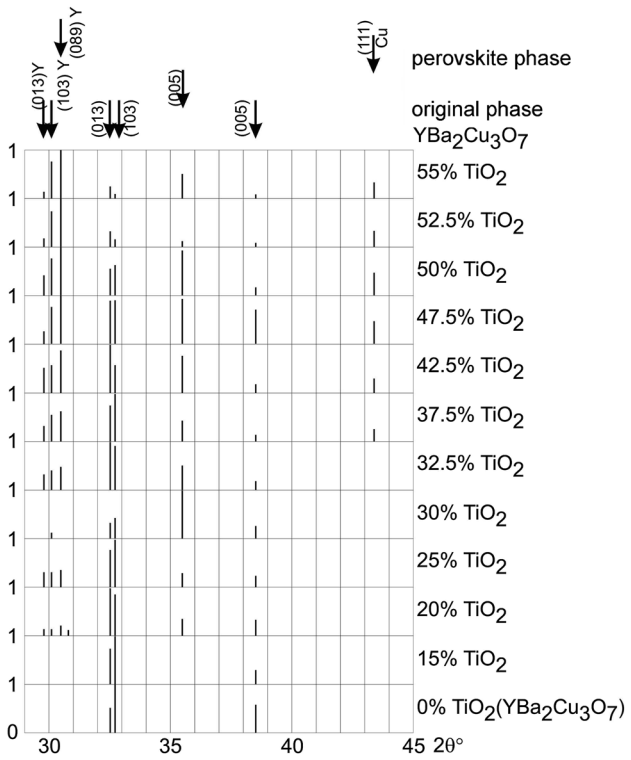

Fig. 1 Phase composition in the Ti-doped $YBa_2Cu_3O_{7-\delta}$ samples with increasing nominal Ti content

allowed to obtain a transient contact resistance of less than 1 Ω. The measurements were done in the regime of temperature sweeps. Temperature was measured by a platinum thermoresistor, while the voltage by 2–38 nanovoltmeters. The transition temperature was determined at the point of maximum in the dependences $dR(T)/dT$ in the region of the superconducting transition. Magnetic fields up to 7 T were created by a superconducting solenoid.

The resistive transitions into the superconducting state were measured by the Kouvel–Fischer method [19]. This method relies upon the analysis of

$$\chi = \frac{-d(\ln \Delta\sigma)}{dT}, \tag{1}$$

where $\Delta\sigma = \sigma - \sigma_0$ is some correction to the conductivity appearing in the superconducting subsystem in consequence of the fluctuation pairing of the charge carriers at $T > T_c$ [20, 21] and determined by the phase state of the vortex matter at $T < T_c$ [22, 23]. Here $\sigma = \rho^{-1}$ is the experimentally measurable conductivity value and $\sigma_0 = \rho_0^{-1} = (A + BT)^{-1}$ is the regular subtrahend determined by extrapolating the high-temperature linear section down to the superconducting transition region. Assuming that $\Delta\sigma$ diverges as $\Delta\sigma \propto (T - T_c)^{-\beta}$ at $T \approx T_c$, from Eq. (1) follows

$$\chi^{-1} = \beta^{-1}(T - T_c), \tag{2}$$

where β is some exponent depending on the dimensionality and the phase state of the fluctuational and the vortex subsystem [18, 20–23]. In this way, the identification of the linear temperature sections in the dependences $\chi^{-1}(T)$ allows one to simultaneously determine the dimensional exponents and the characteristic temperature of the dynamical phase transitions in the subsystem of superconducting charge carriers.

3 Results and discussion

Figure 2 displays the temperature dependences of the electrical resistance in the basal plane $R \equiv R_{ab}$ of the sample with the nominal 30 at.% Ti content at a series of magnetic fields up to 7 T. In the broad temperature range, with decreasing temperature from 300 K $R(T)$ decreases nearly linearly down to some characteristic temperature $T^* \approx 153$ K. Below this temperature the experimental data begin to systematically deviate down from the linear dependence. This is a consequence of the excess conductivity introduced in the previous subsection. According to the contemporary views, such a behavior of $R(T)$ at temperatures $T \gg T_c$ is caused by the so-called pseudogap anomaly, as discussed e.g. in Ref. [12].

The application of the magnetic field does not affect the curves $R(T)$ above the superconducting transition, within the accuracy of the experiment. Simultaneously, with increasing magnetic field the superconducting transitions are broadening as compared with a rather sharp transition at $H = 0$ for which $\Delta T_c \simeq 1.5$ K. One should also emphasize the substantial difference in the shape of the resistive transitions for the Ti-doped sample studied here from the curves of impurity-free samples [7, 24] in a magnetic field. Whereas in the latter case one observes a sharp kink in the "tail" of the superconducting transition, in our case a monotonic smoothing of the low-temperature part of the resistive transition takes place. The latter is reflected in the disappearance of the low-temperature peak in the temperature dependences of the derivatives $dR(T)/dT$ in Fig. 3. As is known from literature [13, 18], the appearance of such peculiarities in the temperature dependence $R(T)$ and $dR(T)/dT$ attests to the realization in the system of a first-order phase transition corresponding to the vortex lattice melting. The disappearance of the mentioned peculiarities in the case of Ti doping might attest to a suppression of this transition. At the same time, it should be noted that in our case the resistive transitions exhibit some universal dependence, running over the slope located on the left from the main, high-temperature peak in the dependence $dR(T)/dT$.

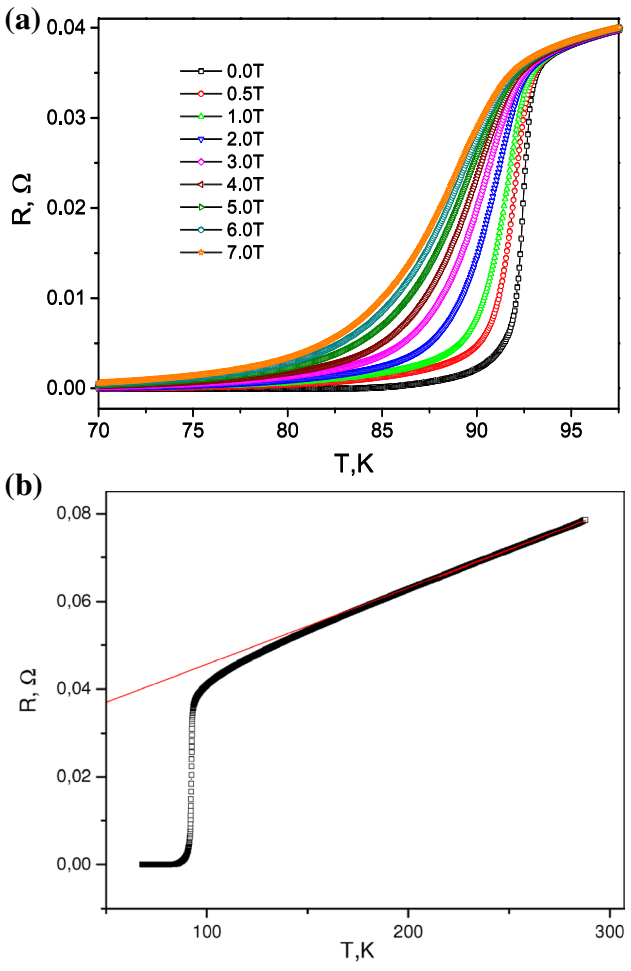

Fig. 2 Temperature dependences of the electrical resistance $R(T)$ of the $YBa_2Cu_3O_{7-\delta}$ sample with the nominal 30 at.% Ti content before (**a**) and after (**b**) reducing the oxygen content for $H = 0$ (curve 1) and for = 0–7 T—curves 2–9, respectively. The *dashed line* depicts the extrapolation of the linear section to the low-temperature region

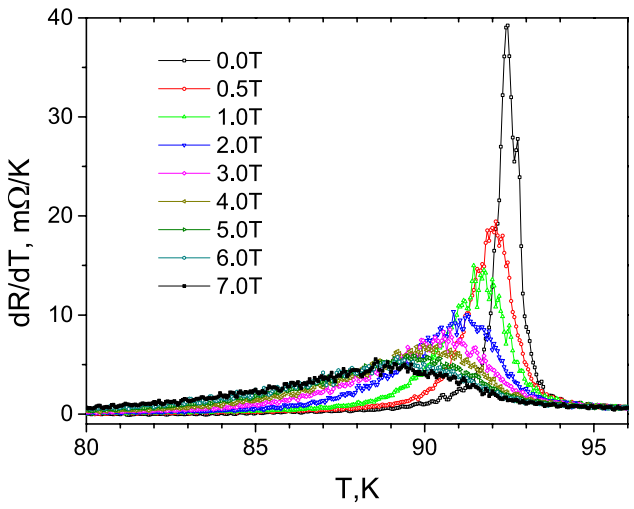

Fig. 3 Transitions into the superconducting state of the $YBa_2Cu_3O_{7-\delta}$ sample with the nominal 30 at.% Ti content in dR/dT versus T representation. Curve numbering is the same as in Fig. 2

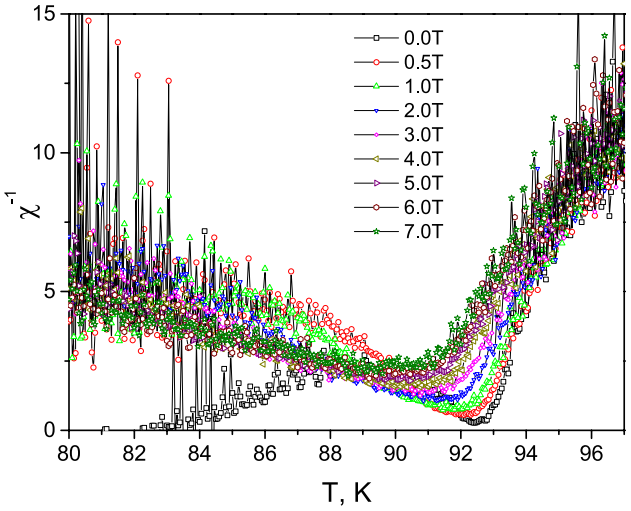

Fig. 4 Transitions into the superconducting state of the $YBa_2Cu_3O_{7-\delta}$ sample with the nominal 30 at.% Ti content in $[\frac{-d(\ln \Delta\sigma)}{dT}]^{-1}$ versus T representation. Curve numbering is the same as in Fig. 2

According to Ref. [22], the temperature associated with this peak corresponds to the critical temperature in the mean-field approximation T_c^{mf}. This, in turn, may attest to the realization of some new state of the conducting subsystem.

The resistive transitions to the superconducting state are shown in Fig. 4 in $[\frac{-d(\ln \Delta\sigma)}{dT}]^{-1}$ versus T representation. One sees that in the high-temperature region of the superconducting transition all curves exhibit an extended linear section with the slope $\beta \approx 0.5$ that according to Ref. [20] attests to the realization in the system of the 3D regime for the fluctuational carriers. The section corresponding to the 3D regime is substantially unstable in the magnetic field, that is in agreement with the results reported in Ref. [18]. Further away from T_c towards higher temperatures a further increase of β takes place. This may attest to the realization in the system of the 3D–2D crossover [20, 21].

The application of the magnetic field leads to a substantial broadening and smearing of the superconducting transition. As is known from literature [17, 24], to this effect can lead the presence in the system of active pins contributing to the kink smearing and leading to a transition of the phase of a disordered vortex lattice to the vortex glass phase. This phase is stipulated by the adaptation of the vortex system to the random pinning potential. In other words, the random pinning destroys the long-range order of the vortex lattice, thereby suppressing the first-order phase transition and stimulating the realization of the vortex glass phase [17]. In consequence of this, "tails" appear in the resistance. Their magnitude is smaller than the flux–flow resistance ρ_{ff} that is likely caused by a partial pinning of the vortex liquid.

In our case the pinning potential is induced by grain boundaries and phase inclusions associated with the titanium doping. The latter assumption is corroborated by the results of the X-ray inspection along with the fact that effect of "kink smearing" is not often observed in samples from the 1–2–3 system without titanium [5, 24] or with impurities leading to the full or a partial substitution of the original components [22]. In this way, one can assume that in the investigated sample coexist a pinning potential induced by grain boundaries and the volume pinning owing to the order parameter suppression induced by the titanium impurities.

As it was shown in Ref. [18], in the $\chi(T)$ dependence in the vortex glass state one should observe a scaling in the reduced $(T_c - T_{c_0})$ versus $(T - T_{c_0})/(T_c - T_{c_0})$ coordinates, where T_{c_0} is the critical temperature of the end of the transition in the paracoherent region. The temperature T_{c_0} is determined at the intersection point of the linear dependence approximating the so-called paracoherent region with the temperature axis. The temperature T_c is the temperature corresponding to the mean-field critical temperature determined at the point of maximum in the dependences $dR(T)/dT$.

In Fig. 5 are plotted the curves scaled as $(T_c - T_{c_0})/\varepsilon_\alpha$ versus $(T - T_{c_0})/(T_c - T_{c_0})$. One sees that for the experimental curves the best scaling is observed in the paracoherent region at $T < T_c$. At higher temperatures scattering of the curves becomes more pronounced. This is likely caused by the effect of pinning of the superconducting fluctuations to the phase inclusions and the possible enhancement of the role of specific mechanisms of the quasiparticle interaction [25–29].

To sum up, near T_c the fluctuation conductivity is satisfactory described by the 3D Aslamazov–Larkin model

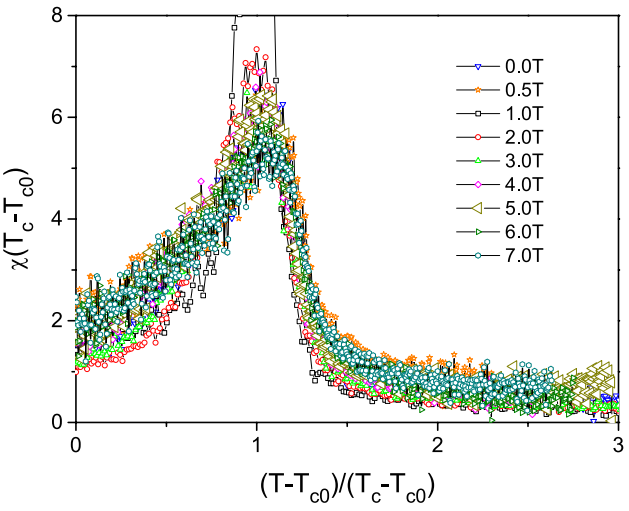

Fig. 5 Transitions into the superconducting state of the $YBa_2Cu_3O_{7-\delta}$ sample with the nominal 30 at.% Ti content in $\chi(T_c - T_{c_0})$ versus T representation. Curve numbering is the same as in Fig. 2

for layered cuprate systems. The application of steady magnetic fields to the $YBa_2Cu_3O_{7-\delta}$ with Ti impurities, in contrast to analogoues impurity-free samples, leads to a smearing of the additional paracoherent transition in the temperature dependences of the excess conductivity in the basal plane in the region of the superconducting transition. This can be a consequence of the effect of the volume pinning stipulated by the presence in the system of phase inclusions due to the Ti doping. For this reason, at temperatures below the critical temperature $T < T_c$ the dynamical phase transition of the vortex liquid–vortex lattice type is suppressed and the transition of the vortex liquid–vortex glass phase takes place.

References

1. J. Bednorz, K. Müller, Z. Phys. B **64**(2), 189–193 (1986)
2. T.A. Friedmann, J.P. Rice, J. Giapintzakis, D.M. Ginsberg, Phys. Rev. B **39**, 4258–4266 (1989)
3. R. Vovk, G. Khadzhai, I. Goulatis, A. Chroneos, Physica B **436**, 88–90 (2014)
4. A. Solovjov, M. Tkachenko, R. Vovk, A. Chroneos, Physica C **501**, 24–31 (2014)
5. G. Blatter, M.V. Feigel'man, V.B. Geshkenbein, A.I. Larkin, V.M. Vinokur, Rev. Mod. Phys. **66**, 1125–1388 (1994)
6. R.V. Vovk, N.R. Vovk, O.V. Dobrovolskiy, J. Low Temp. Phys. **175**(3–4), 614–630 (2014)
7. A.V. Bondarenko, V.A. Shklovskij, R.V. Vovk, M.A. Obolenskii, A.A. Prodan, Low Temp. Phys. **23**(12), 962–967 (1997)
8. A.V. Bondarenko, V.A. Shklovskij, M.A. Obolenskii, R.V. Vovk, A.A. Prodan, M. Pissas, D. Niarchos, G. Kallias, Phys. Rev. B **58**, 2445–2447 (1998)
9. V.M. Pan, V.L. Svetchnikov, V.F. Solovjov, V.F. Taborov, H.W. Zandbergen, J.G. Wen, Supercond. Sci. Technol. **5**(12), 707 (1992)
10. R.V. Vovk, M.A. Obolenskii, A.A. Zavgorodniy, Z.F. Nazyrov, I.L. Goulatis, V.V. Kruglyak, A. Chroneos, Mod. Phys. Lett. B **25**, 2131–2136 (2011)
11. Z. Li, H. Wang, N. Yang, X. Jin, J. Chin. Ceram. Soc. **18**, 555–560 (1990)
12. S.V. Savich, A.V. Samoilov, R.V. Vovk, O.V. Dobrovolskiy, S.N. Kamchatna, Y.V. Dolgopolova, O.A. Chernovol-Tkachenko, Mod. Phys. Lett. B **30**(04), 1650034 (2016)
13. M.K. Wu, J.R. Ashburn, C.J. Torng, P.H. Hor, R.L. Meng, L. Gao, Z.J. Huang, Y.Q. Wang, C.W. Chu, Phys. Rev. Lett. **58**, 908–910 (1987)
14. B. Martínez, F. Sandiumenge, S.P. nol, N. Vilalta, J. Fontcuberta, X. Obradors, Appl. Phys. Lett. **66**(6), 772–774 (1995)
15. R. Vovk, N. Vovk, A. Samoilov, I. Goulatis, A. Chroneos, Solid State Commun. **170**, 6–9 (2013)
16. T. Kemin, H. Meisheng, W. Yening, J. Phys. **1**(6), 1049 (1989)
17. R.V. Vovk, Z.F. Nazyrov, M.A. Obolenskii, I.L. Goulatis, A. Chroneos, V.M. Pinto Simoes, J. Alloys Compd. **509**(13), 4553–4556 (2011)
18. R.M. Costa, I. Riegel, A. Jurelo, J. Pimentel Jr., J. Magn. Magn. Mater. **320**(14) e493–e495 (2008). VIII Latin American Workshop on Magnetism, Magnetic Materials and their Applications
19. J.S. Kouvel, M.E. Fisher, Phys. Rev. **136**, A1626–A1632 (1964)
20. L.G. Aslamasov, A.I. Larkin, Phys. Lett. A **26**(6), 238–239 (1968)
21. R.V. Vovk, N.R. Vovk, G.Y. Khadzhai, O.V. Dobrovolskiy, Z.F. Nazyrov, Curr. Appl. Phys. **14**(12), 1779–1782 (2014)
22. J. Roa-Rojas, R. Menegotto Costa, P. Pureur, P. Prieto, Phys. Rev. B **61**, 12457–12462 (2000)
23. R.V. Vovk, V.M. Gvozdikov, M.A. Obolenskii, Z.F. Nazyrov, V.V. Kruglyak, Acta Phys. Pol. A **121**, 1191–1194 (2012)
24. W.K. Kwok, S. Fleshler, U. Welp, V.M. Vinokur, J. Downey, G.W. Crabtree, M.M. Miller, Phys. Rev. Lett. **69**, 3370–3373 (1992)
25. R.V. Vovk, G.Y. Khadzhai, O.V. Dobrovolskiy, Appl. Phys. A **117**, 997–1002 (2014)
26. V.N. Golovach, M.E. Portnoi, Phys. Rev. B **74**, 085321 (2006)
27. R.V. Vovk, Z.F. Nazyrov, I.L. Goulatis, A. Chroneos, Physica C **485**, 89–91 (2013)
28. U. Schwingenschlögl, C. Schuster, Appl. Phys. Lett. **100**(25), 2130 (2012)
29. P.J. Curran, V.V. Khotkevych, S.J. Bending, A.S. Gibbs, S.L. Lee, A.P. Mackenzie, Phys. Rev. B **84**, 104507 (2011)